Electronic Supplementary Material (ESI).
This journal is © The Royal Society of Chemistry 2021

Electronic Supplementary Information

Endowing Organic Nitro-Compounds with Bright and Stimuli-Sensitive Luminescence Based on Propeller-Like AIEgens

Riqing Ding, ‡[a] Ke Qin, ‡[a] Huili Sun , ‡[a] Shasha Zhou,[a] Sidan Guo,[a] Hui Feng,[a] Huili Ma*[bc] and Zhaosheng Qian*[a]

Table of Contents

1. Experimental Section

Synthesis of (*E*)-1,2-Di(*1H*-indol-1-yl)-1,2-bis(4-nitrophenyl)ethene (DIBNPE). A certain amounts of indole (1.17 g, 10 mmol) and 4-nitrobenzyl bromide (3.24 g, 15 mmol) were dissolved in 80 mL DMSO, and then 3.36 g of KOH was added. The mixture was stirred at room temperature in the dark for 30 hours. After the reaction was completed, 50 mL of water was added into the above mixture. The product was extracted with dichloromethane (150 mL) three times, and further purified through a silica gel column using petroleum ether and dichloromethane as the eluent. The pure product was finally obtained as an orange solid (Yield 17%). Molecular formula: $C_{30}H_{20}N_4O_4$. ^{1}H NMR(600 MHz, $CDCl_3$) δ (ppm) 7.93(d, J = 8 Hz, 4H), 7.64(d, J = 8 Hz, 2H), 7.14(t, J = 7 Hz, 2H), 7.06(t, J = 7 Hz, 2H), 6.98(d, J = 7 Hz, 4H), 6.92(d, J = 7 Hz, 2H), 6.84(d, J = 7 Hz, 2H), 6.66(d, J = 7 Hz, 2H). ^{13}C NMR (150 MHz, $CDCl_3$) δ(ppm) 141.67, 135.81, 132.80, 128.91, 128.73, 123.93, 123.26, 121.62, 121.49, 106.34, 99.98. HRMS (ESI) m/z $[M+H]^+$ 501.1531, $[M+Na]^+$ 523.1348, $[M+K]^+$ 539.1086 (calcd. for $C_{26}H_{16}Cl_4$, 500.1485).

Synthesis of (*E*)-1,2-Di(*9H*-carbazol-9-yl)-1,2-bis(4-nitrophenyl)ethene (DCBNPE). A certain amounts of carbzaole (1.67 g, 10 mmol) and 4-nitrobenzyl bromide (3.24 g, 15 mmol) were dissolved in 80 mL DMSO, and then 3.36 g of KOH was added. The mixture was stirred at room temperature in the dark for 30 hours. After the reaction was completed, 50 mL of water was added into the above mixture. The product was extracted with dichloromethane (150 mL) three times, and further purified through a silica gel column using petroleum ether and dichloromethane as the eluent. The pure product was finally obtained as an orange-red solid (Yield 23%). Molecular formula: $C_{38}H_{24}N_4O_4$. ^{1}H NMR(600 MHz, $CDCl_3$) δ (ppm) 8.47(d, J = 8 Hz, 4H), 8.14(d, J = 6 Hz, 4H), 7.78(d, J = 8 Hz, 4H), 7.49(d, J = 8 Hz, 4H), 7.44(t, J = 8 Hz, 4H), 7.34(t, J = 8 Hz, 4H). ^{13}C NMR (150 MHz, $CDCl_3$) δ(ppm) 147.86, 142.35, 139.64, 132.70, 128.54, 126.85, 124.65, 124.22, 121.59, 121.03, 110.99. HRMS (ESI) m/z: $[M+H]^+$ 601.1841,

$[M+NH_4]^+$ 618.2112, $[M+Na]^+$ 623.1659, $[M+K]^+$ 639.1401 (calcd. for $C_{38}H_{24}N_4O_4$, 600.6216).

Characterization of Fluorescence Properties of All Samples. Steady PL spectra of all samples were performed on an Edinburgh Instruments model FLS980 fluorescence spectrophotometer equipped with a xenon arc lamp using a front face sample holder. Time-resolved fluorescence measurements were conducted with EPL-series lasers. The fluorescence quantum yields of all samples were determined using an integrating sphere equipped in FLS980 spectrophotometer for at least three times.

2. Computational Details

2.1 Electronic structures

The equilibrium geometries and normal modes for ground (S_0) and the lowest singlet excited states (S_1) of all the two compounds were evaluated by using (TD)B3LYP functional together with 6-31+G(d, p) basis set.[1] Bulk solvent effects have been included using polarizable continuum model (PCM).[2] Based on the optimized S_1-geometry, the excitation energies and natural transition orbitals (NTOs) of the low-lying excited states were calculated at TD-BMK/6-31+G(d,p) level by using Gaussian 09 program[3], while the corresponding spin-orbit coupling matrix elements were produced by interfaced with PySOC code[4]. The reduced density gradient isosurface[5] and electrostatic potential were simulated based on S_0-geometry by using Multiwfn package.[6]

2.2 The Lippert-Mataga model

The change in magnitude of the dipole moment between the ground and excited states, that is, $\Delta\mu = |\mu_e - \mu_g|$ can be estimated using the Lippert–Mataga equation[7]

$$hc(\upsilon_a - \upsilon_f) = hc(\upsilon_a^0 - \upsilon_f^0) + \frac{2(\mu_e - \mu_g)^2}{a_0^3} f(\varepsilon,n)$$

where μ_e is the dipole moment of excited state, μ_g is the dipole moment of ground state, h is the Plank constant, c is the light speed in vacuum, a_0 is the solvent Onsager cavity radius, is the Stokes shift, and $f(\varepsilon, n)$ is the orientational polarizability of solvents, written as

$$f(\varepsilon,n) = \frac{\varepsilon - 1}{2\varepsilon + 1} - \frac{n^2 - 1}{2n^2 - 1}$$

Where ε is the static dielectric constant and n is the optical refractivity index of the solvent. Through the analysis of the fitted line in low-polarity solvents, its corresponding

μ_e was calculated to be 4.98 D with the slope of 936.04 (R^2= 0.9864) according to Lippert-Mataga equation. However, in high-polarity solvents, the μ_e was increased to 25.04 D with the slope of 30314.15 (R^2= 0.8924).

3. Supplementary Schemes and Figures

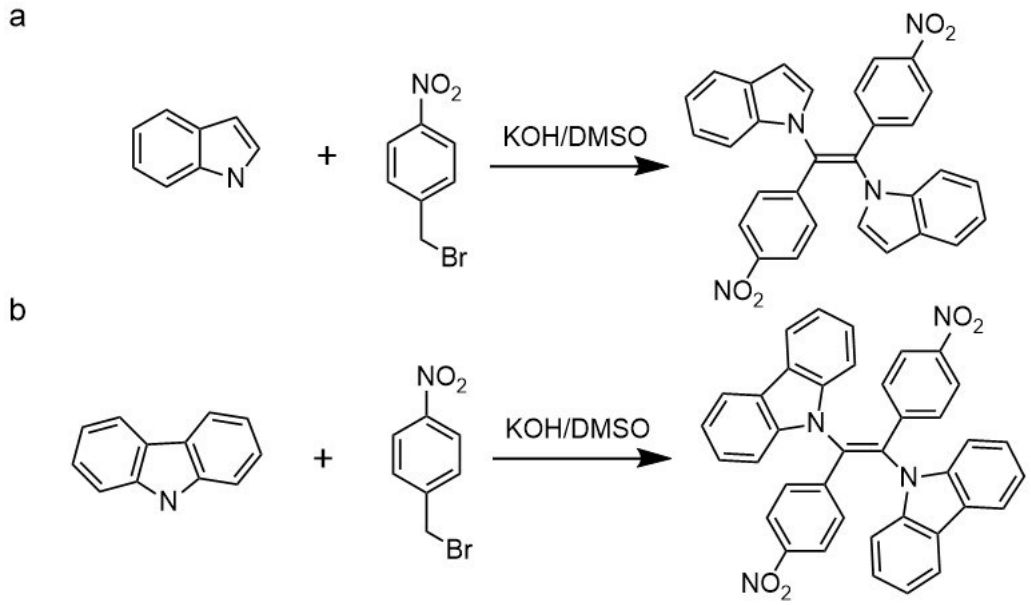

Scheme S1. Synthesis routes of DIBNPE and DCBNPE.

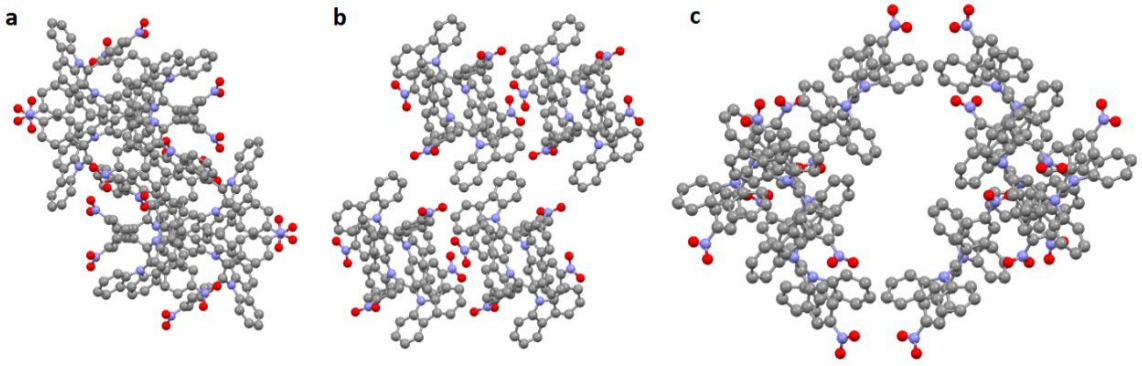

Figure S1. Molecular stacking structures of DCBNPE along the *a*-axis (a), *b*-axis (b) and *c*-axis (c) directions in the crystal (CCDC no. 1969990). Hydrogen atoms are omitted for clarity.

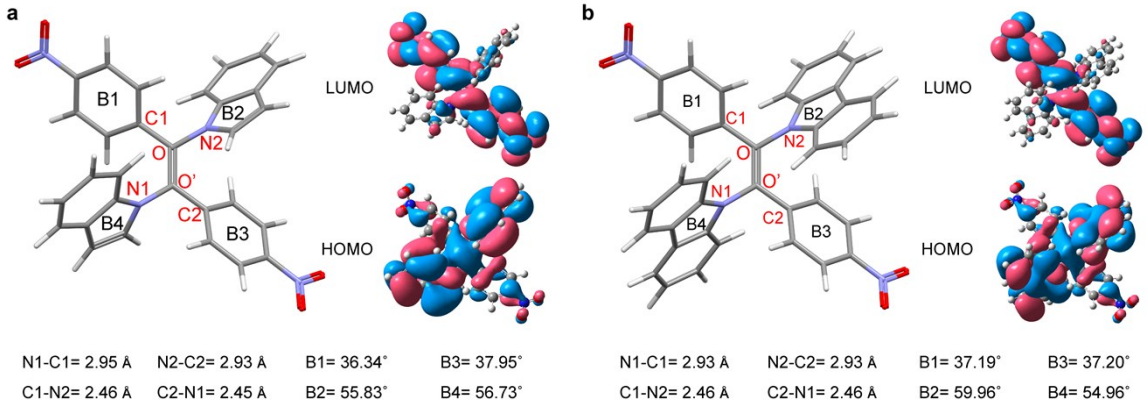

Figure S2. (a) Calculated C−N distances and twisting angle between phenyl and indolyl/carbazole rings in DCBNPE and DIBNPE. (b) Electron cloud distributions of DCBNPE and DIBNPE in the ground states. Set (C1−N2−O) as the reference plane when calculated the twisting angle of phenyl rings B1 and B2. Set (N1−C2−O') as the reference plane when calculated the twisting angle of phenyl rings B3 and B4.

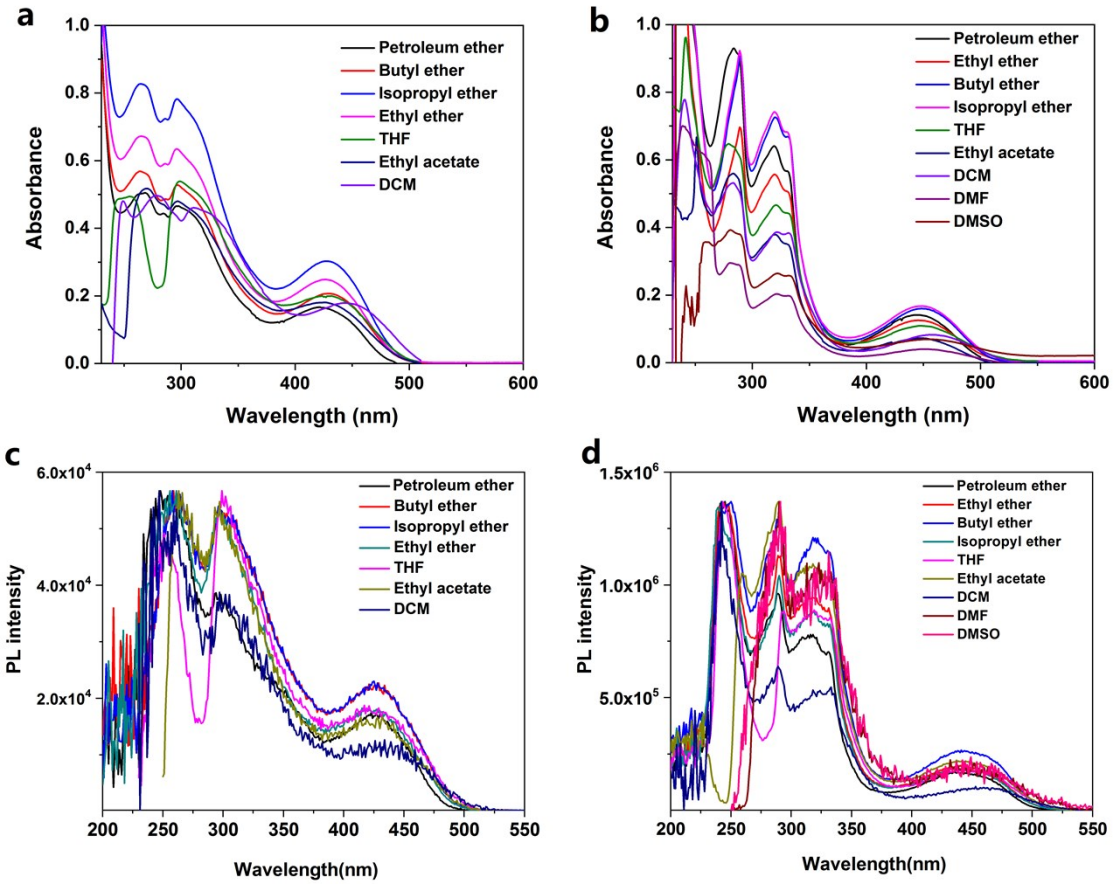

Figure S3. UV-visible spectra of DIBNPE (a) and DCBNPE (b) in various solvents, and excitation spectra of DIBNPE (c) and DCBNPE (d) in various solvents.

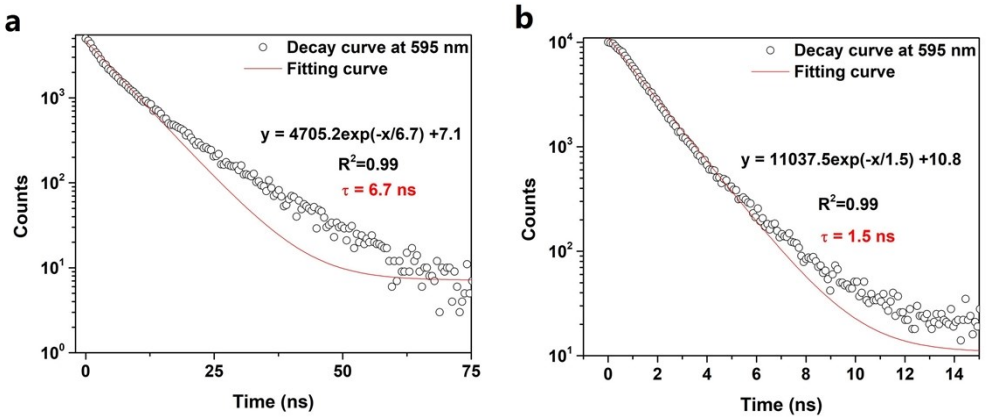

Figure S4. Time-resolved PL decay curves of DIBNPE in THF (a) and in solid (b).

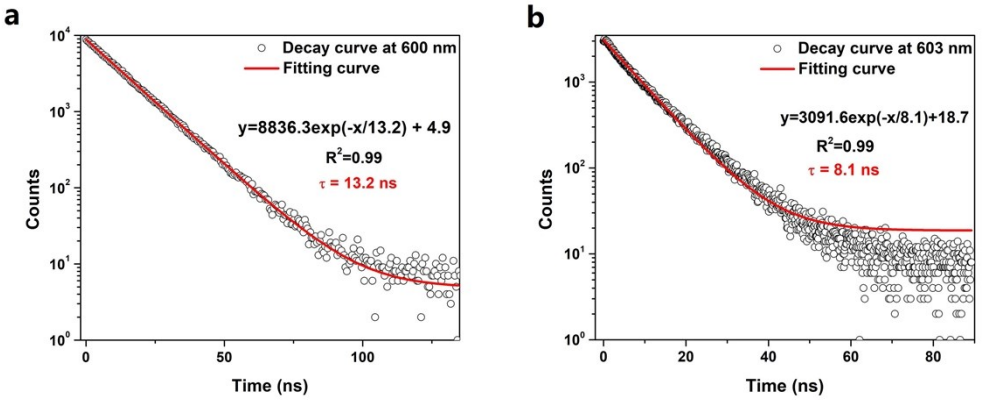

Figure S5. Time-resolved PL decay curves of DCBNPE in THF (a) and in solid (b).

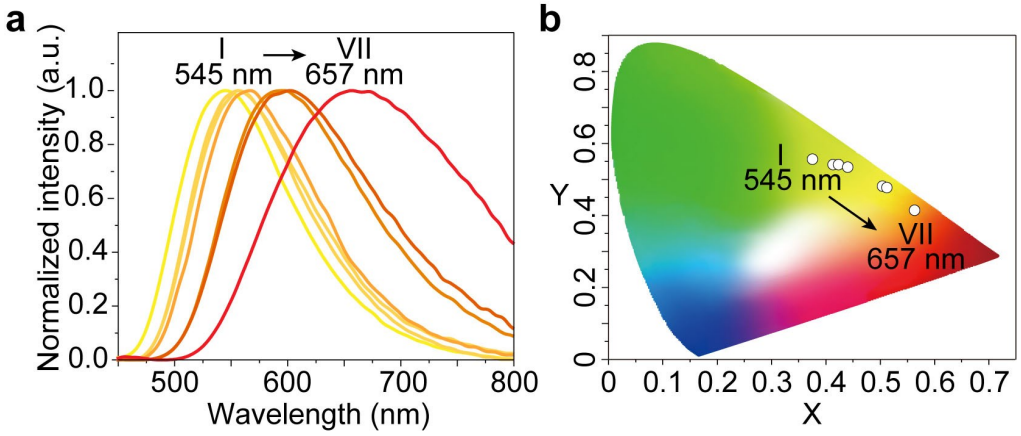

Figure S6. (a) Photophysical properties of DIBNPE (50.0 μM) in diverse organic solvents (I: Petroleum ether, II: Butyl ether, III: Isopropyl ether, IV: Ethyl ether, V: THF, VI: Ethyl acetate, VII: DCM). a) PL spectra of DIBNPE. (b) CIE chromaticity coordinate variation of the fluorescence emission colors of DIBNPE with changing organic solvents from I to IX.

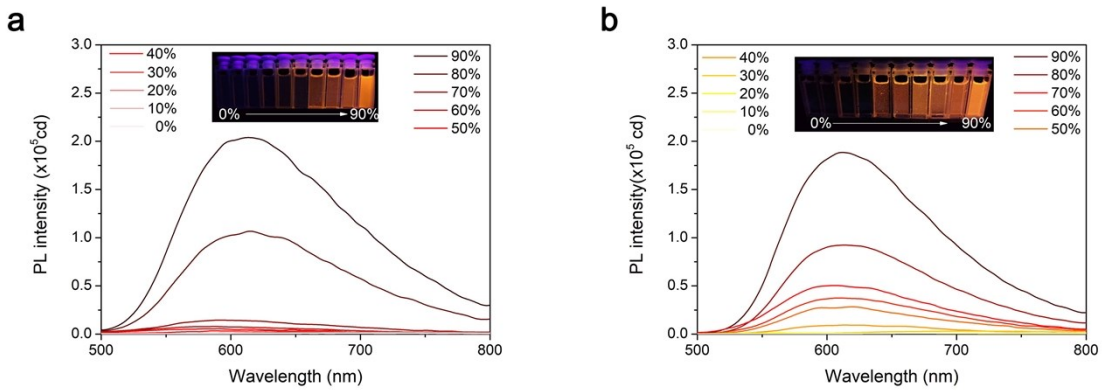

Figure S7. PL spectra of DIBNPE(a) and DCBNPE(b) in DMSO with increase of water fractions (vol%).

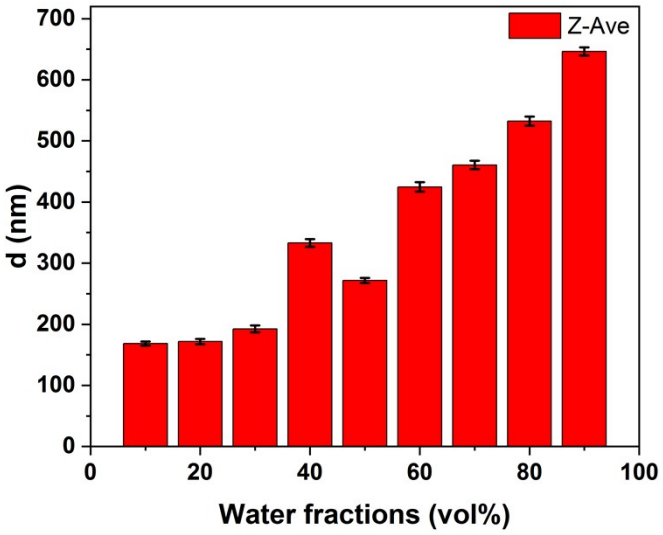

Figure S8. Size distribution of DCBNPE in DMSO with the increase of water fraction (vol%) measured by dynamic light scattering technique.

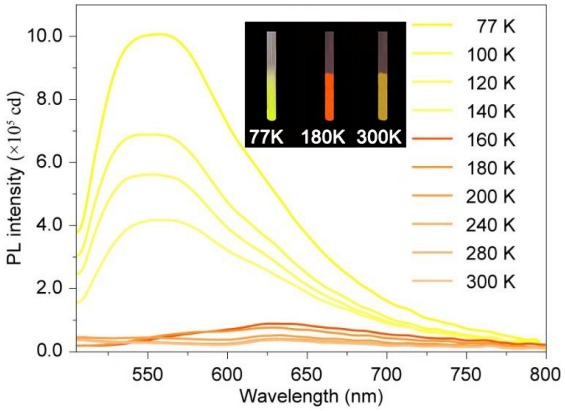

Figure S9. Temperature-dependent PL spectra of DIBNPE from 77 to 300 K in THF.

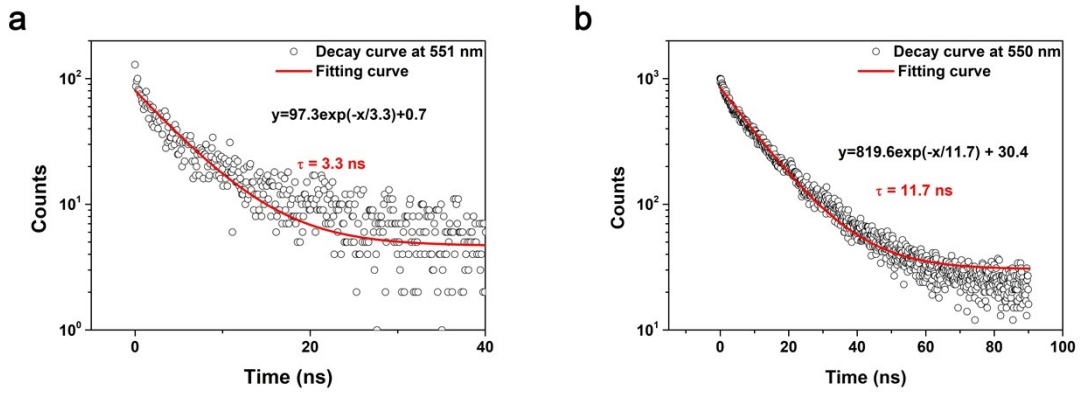

Figure S10. Time-resolved PL spectra of DIBNPE (a) and DCBNPE (b) in THF at 77 K.

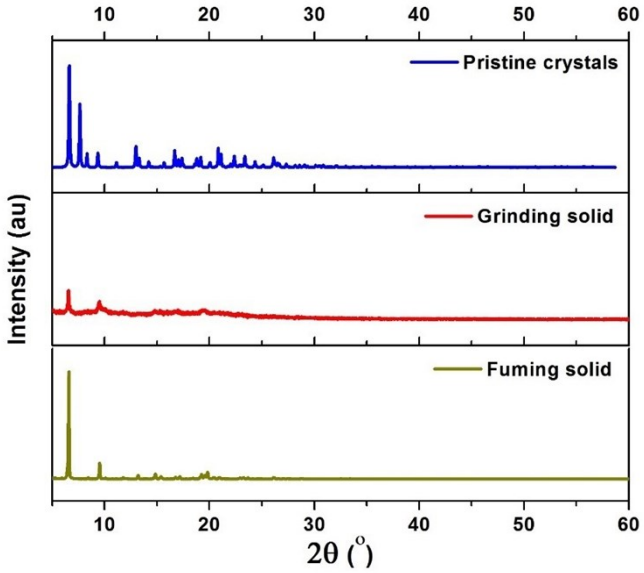

Figure S11. XRD patterns of pristine crystals, ground solid and fuming solid of DCBNPE.

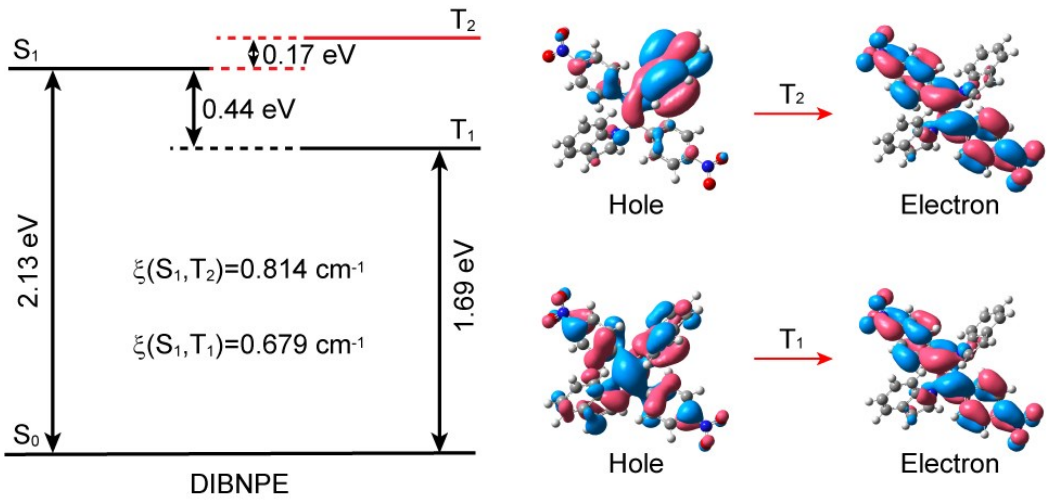

Figure S12. Energy diagrams, spin-orbit coupling matrix elements (ξ) and natural transition orbitals (NTOs) of the low-lying excited states for DIBNPE.

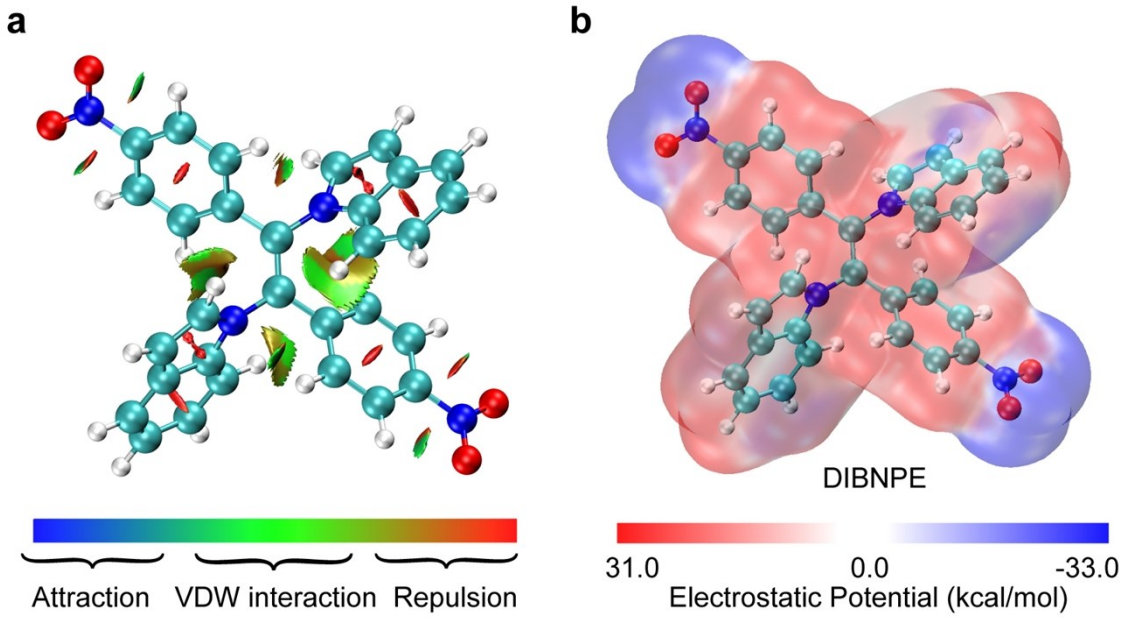

Figure S13. (a) The reduced density gradient (RDG) isosurface map with an isovalue of 0.5 for DIBNPE. (b) Electrostatic potential on the 0.001 au molecular surface of DIBNPE.

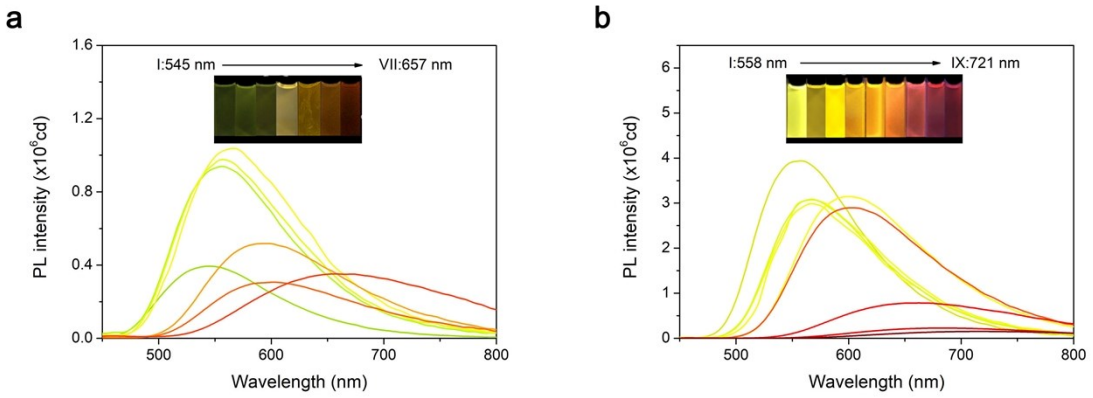

Figure S14. Photophysical properties of DIBNPE in diverse organic solvents (I: Petroleum ether, II: Butyl ether, III: Isopropyl ether, IV: Ethyl ether, V: THF, VI: Ethyl acetate, VII: DCM). Solvatochromism of DIBNPE(a) and DCBNPE(b) Insets: fluorescence images in different solvents.

4. Supplementary Tables

Table S1. Crystallographic data for DCBNPE

source	DCBNPE
CCDC No.	1969990
chemical formula	$C_{38}H_{24}N_4O_4$
formula weight	600.62
temperature (K)	301
wavelength (Å)	1.54178
crystal system	monoclinic
space group	C 1 2/c 1
a (Å)	28.467(4)
b (Å)	12.8462(17)
c (Å)	20.218(3)
α	90.00
β	110.66
γ	90.00
volume (Å^3)	6917.9
Z	8
no. reflections collected	6342
no. unique reflections	4806
R_{int}	0.994
no. parameters	424
GOF on F^2	1.057
R1	0.0652
wR2	0.2019

Table S2. Detailed photophysical properties of DCBNPE in different solvents.

Solvents	$f(\varepsilon, n)$	λ_a (nm)	λ_e (nm)	ν_a-ν_f (cm_{-1})	Φ_{PL} (%)
Petroleum ether	0.004	444	558	4539.74	95.0
Butyl ether	0.096	449	567	4637.93	72.5
Isopropyl ether	0.145	449	568	4669.00	74.6
Ethyl ether	0.167	446	560	4567.23	78.4
THF	0.21	449	600	5608.55	75.9
Ethyl acetate	0.2	447	607	5900.58	70.2
DCM	0.217	455	658	6784.69	19.2
DMF	0.276	450	682	7564.19	5.5
DMSO	0.264	455	721	8094.19	3.7

Table S3. Photophysical properties of DIBNPE and DCBNPE in THF and in solid.

	λ_{ab} (nm)	ε ($\times 10^4$ L mol^{-1} cm^{-1})	λ_{em} (nm)	τ (ns)	ϕ (%)
		In THF			
DIBNPE	296, 428	3.6, 0.8	595	6.7	5.4
DCBNPE	320, 450	9.4, 0.8	600	13.2	75.9
		In Solid			
DIBNPE	-	-	595	1.5	8.5
DCBNPE	-	-	605	8.1	38.5

Table S4. Photoluminescence properties of DIBNPE in various organic solvents

Solvents	**λ_{em} (nm)**	**τ (ns)**	**ϕ (%)**	**k_r (10^7 s^{-1})**	**k_{nr} (10^7 s^{-1})**
Petroleum ether	554	5.4	4.1	0.8	17.7
Butyl ether	555	1.0	9.8	9.8	90.2
Isopropyl ether	560	1.0	10.2	10.2	89.8
Ethyl ether	561	0.9	10.8	12.0	99.1
THF	595	6.7	5.4	0.9	16.0
Ethyl acetate	600	3.7	3.2	0.9	26.1
DCM	660	4.6	4.0	0.9	20.8
Acetone	-	-	-	-	-
DMF	-	-	-	-	-
DMSO	-	-	-	-	-

Table S5. Photoluminescence properties of DCBNPE in various organic solvents

Solvents	**λ_{em} (nm)**	**τ (ns)**	**ϕ (%)**	**k_r (10^7 s^{-1})**	**k_{nr} (10^7 s^{-1})**
Petroleum ether	558	14.9	95.0	6.4	0.3
Ethyl ether	560	15.9	78.4	4.9	1.4
Butyl ether	567	14.8	72.5	4.9	1.9
Isopropyl ether	568	15.7	74.6	4.8	1.6
THF	600	13.2	75.9	5.8	1.4
Ethyl acetate	607	12.3	70.2	5.7	2.4
DCM	658	2.8	19.2	6.9	28.8
DMF	682	5.8	5.5	0.9	16.3
DMSO	721	2.3	3.7	1.6	41.9

Table S6. Lifetimes of DIBNPE and DCBNPE in DMSO with varying water fraction (%)

Water fraction	**τ(DIBNPE) (ns)**	**τ(DCBNPE) (ns)**
0%	-	2.3
10%	-	5.4
20%	-	7.9
30%	-	8.1
40%	-	8.5
50%	0.9	8.6
60%	1.0	8.7
70%	1.7	8.9
80%	1.8	9.2
90%	2.2	9.5

5. Spectra of Compounds

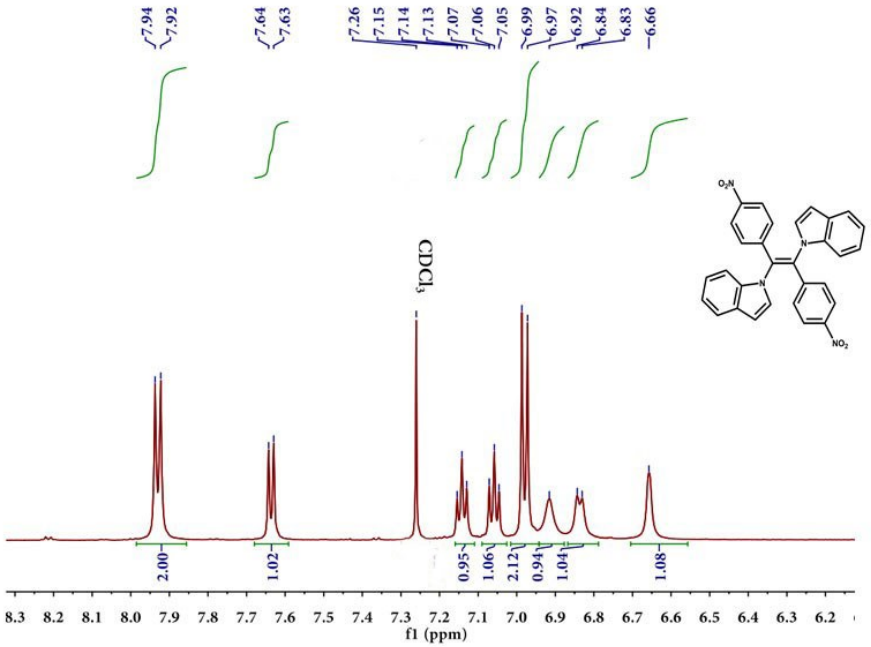

Figure S15. ^{1}H NMR spectrum of (*E*)-1,2-di(*1H*-indol-1-yl)-1,2-bis(4-nitrophenyl)ethene (DIBNPE) in $CDCl_3$

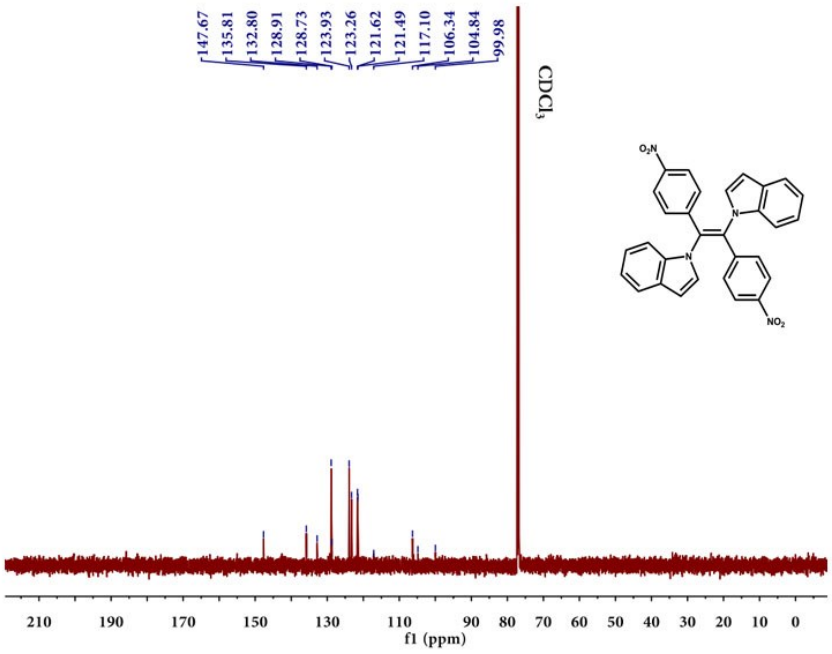

Figure S16. ^{13}C NMR spectrum of (*E*)-1,2-di(*1H*-indol-1-yl)-1,2-bis(4-nitrophenyl)ethene (DIBNPE) in $CDCl_3$

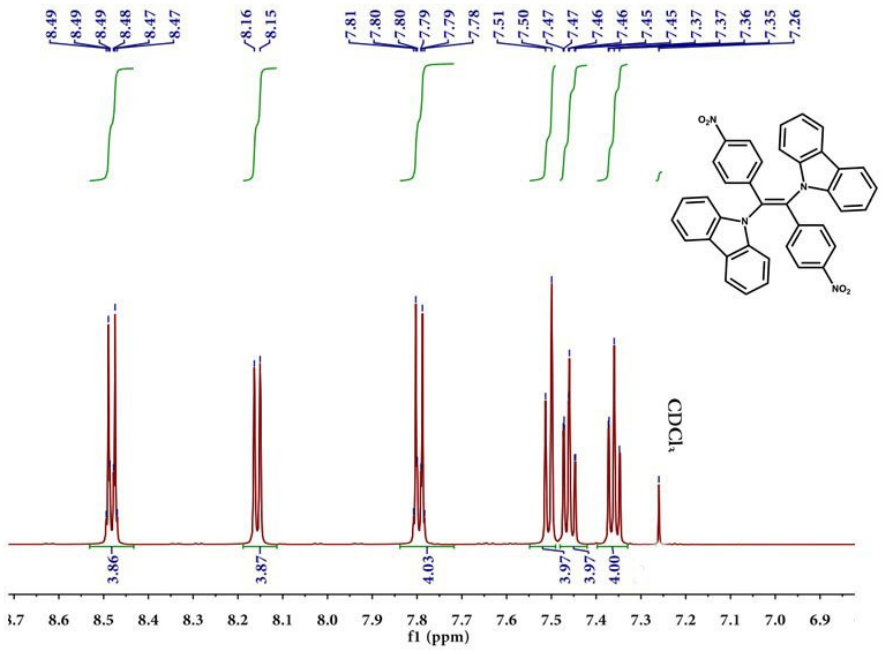

Figure S17. ^{1}H NMR spectrum of (*E*)-1,2-di(*9H*-carbazol-9-yl)-1,2-bis(4-nitrophenyl)ethene (DCBNPE) in $CDCl_3$

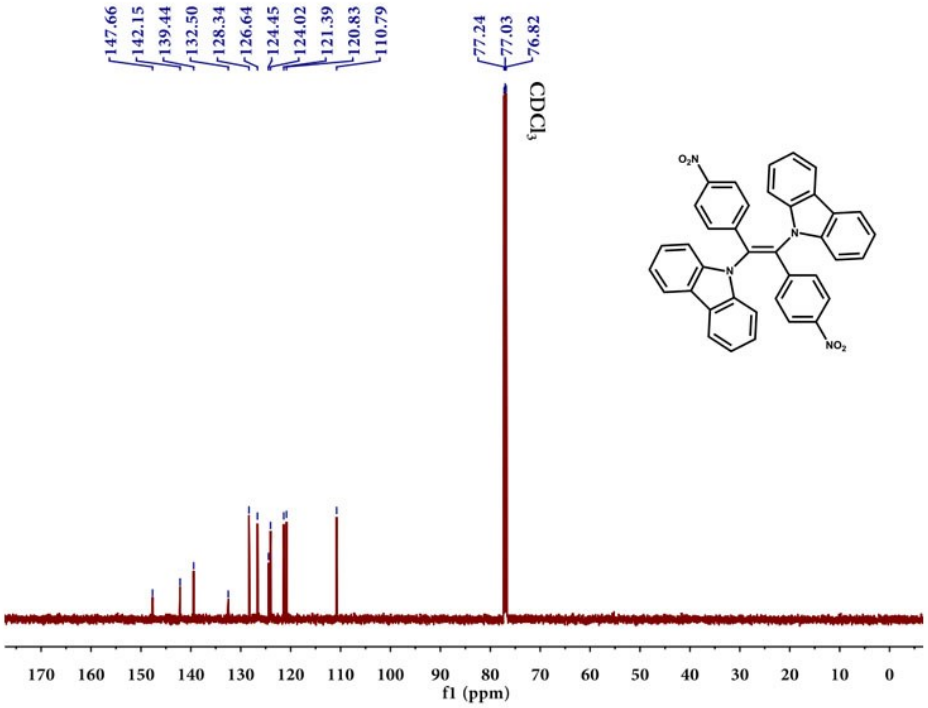

Figure S18. ^{13}C NMR spectrum of (*E*)-1,2-di(*9H*-carbazol-9-yl)-1,2-bis(4-nitrophenyl)ethene in $CDCl_3$

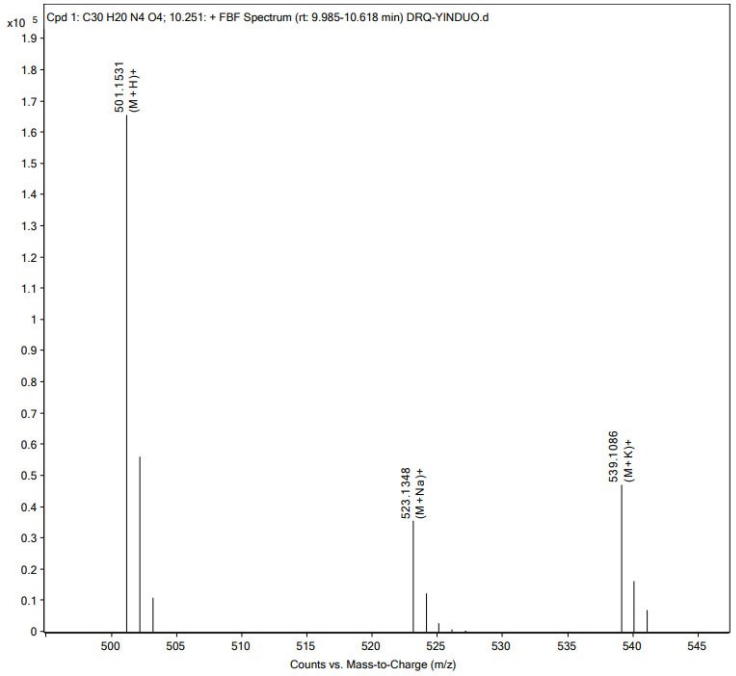

Figure S19. High-resolution mass spectrum of (*E*)-1,2-di(*1H*-indol-1-yl)-1,2-bis(4-nitrophenyl)ethene (DIBNPE)

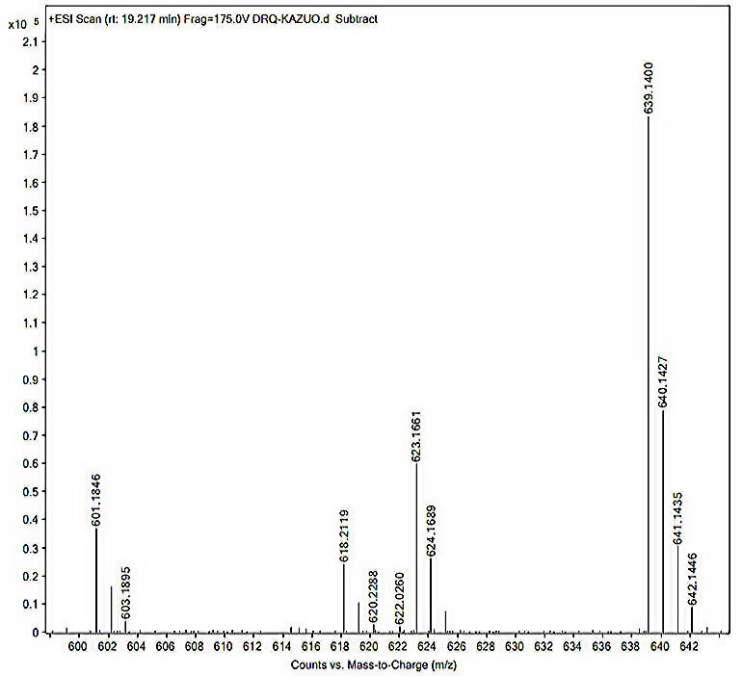

Figure S20. High-resolution mass spectrum of (*E*)-1,2-di(*9H*-carbazol-9-yl)-1,2-bis(4-nitrophenyl)- ethane (DCBNPE)

6. References

(1) Becke, A. D. Density-functional thermochemistry. III. The role of exact exchange. *J. Chem. Phys.* **1993**, *98*, 5648−5652.

(2) Tomasi, J.; Mennucci, B.; Cammi, R. Quantum mechanical continuum solvation models. *Chem. Rev.* **2005**, *105*, 2999−3094.

(3) Frisch, M. J.; Trucks, G. W.; Schlegel, H. B.; Scuseria, G. E.; Robb, M. A.; Cheeseman, J. R.; Scalmani, G.; Barone, V.; Mennucci, B.; Petersson, G. A.; Nakatsuji, H.; Caricato, M.; Li, X.; Hratchian, H. P.; Izmaylov, A. F.; Bloino, J.; Zheng, G.; Sonnenberg, J. L.; Hada, M.; Ehara, M.; Toyota, K.; Fukuda, R.; Hasegawa, J.; Ishida, M.; Nakajiama, T.; Honda, Y.; Kitao, O.; Nakai, H.; Vreven, T.; Montgomery, J. A., Jr.; Peralta, J. E.; Ogliaro, F.; Bearpark, M.; Heyd, J. J.; Borthers, E.; Kudin, K. N.; Staroverov, V. N.; Kobayashi, R.; Normand, J.; Rahavachari, K.; Rendell, A.; Burant, J. C.; Iyengar, S. S.; Tomasi, J.; Cossi, M.; Rega, N.; Millam, J. M.; Klene, M.; Knox, J. E.; Cross, J. B.; Bakken, V.; Adamo, C.; Jaramillo, Gomperts, R.; Stratmann, R. E.; Yazyev, O.; Austin, A. J.; Cammi, R.; Pomelli, C.; Ochterski, J. W.; Martin, R. L.; Morokuma, K.; Zakrzewski, V. G.; Voth, G. A.; Salvador, P.; Dannenberg, J. J.; Dapprich, S.; Daniels, A. D.; Farkas, O.; Foresman, J. B.; Ortiz, J. V.; Cioslowski, J.; Fox, D. J. Gaussian, Inc. Wallingford CT, 2009.

(4) Gao, X.; Bai, S.; Fazzi, D.; Niehaus, T.; Barbatti, M.; Thiel, W. Evaluation of Spin-Orbit Couplings with Linear-Response Time-Dependent Density Functional Methods. *J. Chem. Theory Comput.* 2017, *13*, 515-524.

(5) Johnson, E. R.; Keinan, S.; Mori-Sánchez, P.; Contreras-García, J.; Aron J Cohen, A. J.; Yang W. Revealing noncovalent interactions. *J. Am. Chem. Soc.* 2010, *132*, 6498-6506.

(6) Lu, T.; Chen, F. Multiwfn: A multifunctional wavefunction analyzer. *J. Comput. Chem.* 2012, *33*, 580-592.

(7) Grabowski, Z. R.; Rotkiewicz, K.; Rettig, W. *Chem*. *Rev*. 2003, *103*, 3899–4031.